Available online at www.sciencedirect.com
SCIENCE DIRECT®
Journal of Solid State Chemistry 177 (2004) 633–641
JOURNAL OF SOLID STATE CHEMISTRY
http://elsevier.com/locate/jssc

Hydrothermal syntheses, characterizations and crystal structures of a new lead(II) carboxylate-phosphonate with a double layer structure and a new nickel(II) carboxylate-phosphonate containing a hydrogen-bonded 2D layer with intercalation of ethylenediamines

Jun-Ling Song,[a] Jiang-Gao Mao,[a,*] Yan-Qiong Sun,[a] Hui-Yi Zeng,[a] Reinhard K. Kremer,[b] and Abraham Clearfield[c]

[a] *Fujian Institute for Research on the Structure of Matter, Chinese Academy of Sciences, State Key Laboratory for Structural Chemistry, Fuzhou 350002, People's Republic of China*
[b] *Max-Planck-Institut fuer Festkoerperforschung, Heisenbergstr. 1, D-70569 Stuttgart, Germany*
[c] *Department of Chemistry, Texas A&M University, P.O. Box 30012, College Station, TX 77843-3012, USA*

Received 9 June 2003; received in revised form 11 June 2003; accepted 23 June 2003

Abstract

Hydrothermal reactions of *N*,*N*-bis(phosphonomethyl)aminoacetic acid ($HO_2CCH_2N(CH_2PO_3H_2)_2$) with metal(II) salts afforded two new metal carboxylate-phosphonates, namely, $Pb_2[O_2CCH_2N(CH_2PO_3)(CH_2PO_3H)]\cdot H_2O$ (**1**) and $\{NH_3CH_2CH_2NH_3\}\{Ni[O_2CCH_2N(CH_2PO_3H)_2](H_2O)_2\}_2$ (**2**). Among two unique lead(II) ions in the asymmetric unit of complex **1**, one is five coordinated by five phosphonate oxygen atoms from 5 ligands, whereas the other one is five-coordinated by a tridentate chelating ligand (1 N and 2 phosphonate O atoms) and two phosphonate oxygen atoms from two other ligands. The carboxylate group of the ligand remains non-coordinated. The bridging of above two types of lead(II) ions through phosphonate groups resulted in a $\langle 002 \rangle$ double layer with the carboxylate group of the ligand as a pendant group. These double layers are further interlinked via hydrogen bonds between the carboxylate groups into a 3D network. The nickel(II) ion in complex **2** is octahedrally coordinated by a tetradentate chelating ligand (two phosphonate oxygen atoms, one nitrogen and one carboxylate oxygen atoms) and two aqua ligands. These $\{Ni[O_2CCH_2N(CH_2PO_3H)_2][H_2O]_2\}^-$ anions are further interlinked via hydrogen bonds between non-coordinated phosphonate oxygen atoms to form a $\langle 800 \rangle$ hydrogen bonded 2D layer. The 2H-protonated ethylenediamine cations are intercalated between two layers, forming hydrogen bonds with the non-coordinated carboxylate oxygen atoms. Results of magnetic measurements for complex **2** indicate that there is weak Curie–Weiss behavior with $\theta = -4.4\,K$ indicating predominant antiferromagnetic interaction between the Ni(II) ions. Indication for magnetic low-dimension magnetism could not be detected.

Keywords: Metal phosphonates; Hydrothermal reaction; Layer compounds; Magnetic property; Intercalation

1. Introduction

Metal phosphonate chemistry has attracted a lot of research attention in recent years due to potential applications in the areas of catalysis, ion exchange, proton conductivity, intercalation chemistry, photochemistry, and materials chemistry [1]. Most of the compounds studied are layered species in which the metal octahedra are bridged by phosphonate tetrahedra to form two-dimensional layers that are separated by the hydrophobic regions of the organic moieties. Studies have shown that a variety of metal ions, including group 4 and 14 elements, divalent and trivalent ions, are capable of forming this type of layered compound [1–3]. Besides layered materials, metal phosphonates also exhibit a variety of open framework and microporous structures [1]. Materials with open framework and microporous structures are potential hybrid composite materials in electro-optical and sensing applications in

*Corresponding author. Fax: +865913714946.
E-mail address: mjg@ms.fjirsm.ac.cn (J.-G. Mao).

0022-4596/$ - see front matter © 2003 Elsevier Inc. All rights reserved.
doi:10.1016/j.jssc.2003.06.001

the future [4]. A variety of functional groups such as crown ether, amine and carboxylate groups have been attached to phosphonic acids in search of new inorganic–organic hybrid materials [1,4–16]. Researches on metal complexes with phosphonic acids attached with aza-crown ethers and diaza-crown ethers indicate that those compounds exhibit many unusual structural features such as 1D "macrocyclic leaflets" and microporous 3D networks [1,5,6]. A series of novel pillar layered and microporous materials have been synthesized by hydrothermal reactions of phosphonic acids containing a carboxylate group, such as $H_2O_3PCH_2CH_2CO_2H$ and $H_2O_3PCH_2CO_2H$, with different metal salts [4,7,8]. Studies on metal aminocarboxylate-phosphonates are still relatively rare [9–16]. A new layered zirconium diphosphonate fluoride, $ZrHF(O_3PCH_2)_2NHC_3H_6CO_2$, was reported recently by Vivani et al. [9]. Studies from our group as well as others have shown that *N*-(phosphonomethyl)iminodiacetic acid (H_4PMIDA) is able to form metal phosphonates with 1D chain, 2D layer and 3D porous structures [10–13]. Zinc(II) complex with *N*-(phosphonomethyl)-*N*-methyl glycine have been also reported recently by our group [14a]. Its structure features micropores built from the packing of the unusual heptanuclear zinc(II) carboxylate-phosphonate cluster anions in which the seven Zn(II) ions form a centered octahedron [14a]. Polymeric chains of alkali metal and silver(I) as well as 2D layered Eu(II) complexes with *N*-(phosphonomethyl)-*N*-methyl glycine have also been reported [14b,14c]. An interesting layered Co(II) compound with *N*-(phosphonomethyl)-proline and a layered Pb(II) complex with $HOOCCH_2NHCH_2PO_3H_2$ were also prepared recently [15]. The structure of the zinc(II) *N*,*N*-bis(phosphonomethyl)aminoacetic acid features a 3D network in which the carboxylate and phosphonate groups are bidentate and tridentate bridging, respectively [16a]. A mononuclear Pt(II) complex with *N*,*N*-bis(phosphonomethyl)-aminoacetic acid has also been reported [16b]. In order to understand the effects of different metal ions on the structures of the metal phosphonates formed, we have extended our studies to other divalent transitional and main group metal ions, such as Pb(II) and Sn(II) ions. Studies have shown that the Pb(II) and Sn(II) phosphonates exhibit different structure chemistry from those of transition metal ones due to the presence of the lone pair electrons [17]. Reactions of the *N*,*N*-Bis(phosphonomethyl)-aminoacetic acid with other divalent metal salts afforded two additional new types of metal carboxylate-phosphonate hybrid materials, namely, $Pb_2[O_2CCH_2N(CH_2PO_3)(CH_2PO_3H)]\cdot H_2O$ (**1**), whose structure features a 2D double layer with the carboxylate group as a pendant group, and $\{NH_3CH_2CH_2NH_3\}\{Ni[O_2CCH_2N(CH_2PO_3H)_2](H_2O)_2\}_2$ (**2**), in which the $Ni[O_2CCH_2N(CH_2PO_3H)_2]$ chelating anions are further interlinked by hydrogen bonds between non-coordinated phosphonate oxygen atoms into a hydrogen bonded double layer with the 2H-protonated ethylenediamine being intercalated in-between. Herein we reported their syntheses, characterizations and crystal structures.

2. Experimental section

N,*N*-Bis(phosphonomethyl)aminoacetic acid was prepared by a Mannich type reaction according to procedures described previously [16a]. All other chemicals were obtained from commercial sources and used without further purification. Elemental analyses were performed on a Vario EL III elemental analyzer. Thermogravimetric analyses were carried out with a TGA/SBTA851 unit, at a heating rate of 15°C/min under an oxygen atmosphere. IR spectra were recorded on a Magna 750 FT–IR spectrometer photometer as KBr pellets in the $4000-400\,cm^{-1}$. The XRD powder patterns were collected on a Philips X'Pert-MPD diffractometer using graphite-monochromated Cu$K\alpha$ radiation in the angular range $2\theta = 5-70°$ with a step size of 0.02° and a counting time of 3 s per step. Magnetic measurements in the range of 5–350 K were performed in a MPMS-Squid magnetometer at a field of 1–5 T. The diamagnetic contributions of the cores were corrected by using Pascal's constants.

2.1. Synthesis of $Pb_2[O_2CCH_2N(CH_2PO_3)(CH_2PO_3H)]\cdot H_2O$ 1

A mixture of 1.0 mmol of lead(II) acetate, 0.5 mmol of *N*,*N*-bis(phosphonomethyl)aminoacetic acid and 10.0 mL of deionized water was sealed into a bomb equipped with a Teflon liner, and then heated at 180°C for 5 days. Colorless crystals of complex **1** were recovered in a ca. 45.8% yield. Elemental analysis for complex **1**, $C_4H_9NO_9P_2Pb_2$: C, 6.61; H, 1.66; N, 2.13. Calc. C, 6.95; H, 1.31; N, 2.03%. IR (KBr, cm^{-1}): 3438, 3257, 2912, 1651, 1576, 1409 m, 1232 w, 1054 vs, 917 s, 771 s, 683 w, 563 s, 515 s, 463 m.

2.2. Synthesis of $\{NH_3CH_2CH_2NH_3\}\{Ni[O_2CCH_2N(CH_2PO_3H)_2](H_2O)_2\}_2$ 2

A mixture of 1.0 mmol of $NiCl_2\cdot 6H_2O$, 0.5 mmol of *N*,*N*-bis(phosphonomethyl)aminoacetic acid and 0.5 mmol of 1,2,3-benzenetricarboxylic acid was dissolved in a mixed solvent of 5 mL of deionized water and 5 mL of ethanol. Then the pH value of the resultant solution was adjusted to approximately 6 by slow addition of ethylenediamine. The mixture was sealed into a bomb equipped with a Teflon liner, and then heated at 160°C for 5 days. Green crystals of complex **2**

were recovered in a ca 46.3% yield. Elemental analysis for complex **2**, $C_5H_{17}N_2O_{10}P_2Ni$: C, 15.48; H, 4.68; N, 7.43. Calc. C, 15.56; H, 4.44; N, 7.26%. IR (KBr, cm^{-1}): 3184 s, 2734 s, 2305 m, 1627 s, 1610 s, 1574 vs, 1518 s, 1434 s, 1402 vs, 1336 s, 1254 s, 1203 s, 1173 s, 1137 s, 1105 s, 1087 s, 1074 s, 933 vs, 908 s, 856 m, 783 m, 727 s, 694 m, 599 s, 565 m, 543 m, 489 m, 445 s, 403 w.

3. Crystallography

Single crystals of complexes **1** and **2** were mounted on a Siemens Smart CCD diffractometer equipped with a graphite-monochromated Mo$K\alpha$ radiation ($\lambda = 0.71073$ Å). Intensity data were collected by the narrow frame method at 293 K. The data sets were corrected for Lorentz and polarization as well as for absorption by the SADABS program [18]. Both structures were solved by direct methods and refined by full-matrix least-squares fitting on F^2 by SHELX-97 [18]. All non-hydrogen atoms, except for N(1), C(4), O(11) and O(21) atoms in complex **1**, were refined with anisotropic thermal parameters. All hydrogen atoms except those of the water molecules were located at geometrically calculated positions. Final cycle of refinements reveals featureless residual peak and hole of 2.523 e Å^3 (1.07 Å from Pb(1)) and –3.621 e Å^3 (1.03 Å from Pb(1)) for complex **1**; and 1.260 e Å^3 (1.18 Å from O(23) and –0.761 e Å^3 for complex **2**, respectively. Crystallographic data and structural refinements are summarized in Table 1. Important bond distances and angles are listed in Table 2.

Crystallographic data (excluding structure factors) for the two structures reported in this paper have been deposited with the Cambridge Crystallographic Data Centre as supplementary publication Nos. CCDC 208253 and 208254. Copies of the data can be obtained free of charge on application to CCDC, 12 Union Road, Cambridge CB2 1EZ, UK (fax: +44-1223-336-033; mailto: deposit@ccdc.cam.ac.uk).

4. Results and discussion

The structure of complex **1** features a 2D double layer with the carboxylate group as a pendant group. As shown in Fig. 1, the asymmetric unit of complex **1** contains two unique Pb(II) ions. Pb(1) is five-coordinated by five phosphonate oxygen atoms from five ligands, whereas Pb(2) is five-coordinated by a tridentate chelating ligand (1 N and 2 phosphonate O) and two phosphonate oxygen atoms from two neighboring ligands. The coordination geometry around Pb(1) and Pb(2) ions can be described as a severely distorted square pyramid, the open side of the pyramid is occupied by the lone pair electrons of the Pb(II) ion. The distortion is due to the lone pair electrons of the Pb(II) ion. The Pb–O distances are in the range of 2.38(2)–2.72(2) Å, and the Pb–N bond length is 2.73(2) Å, these distances are comparable to those reported in other lead(II) phosphonates [12b,15b, 17,19]. In addition to the above Pb–O bonds, there are also a number of longer Pb–O contacts (Table 2). These Pb–O distances are in the range of

Table 1
Crystal data and structure refinement for complexes **1** and **2**[a]

Complex	**1**	**2**
Formula	$C_4H_9NO_9P_2Pb_2$	$C_{10}H_{34}N_4O_{20}P_4Ni_2$
Fw	691.44	771.72
Space group	*P*-1 (No. 2)	*C*2/*c* (No. 15)
A (Å)	7.0642(10)	26.5955(10)
b (Å)	7.1478(10)	6.97140(10)
c (Å)	12.0144(17)	15.0818(6)
α (deg)	102.443(2)	90
β (deg)	101.243(2)	109.5930(10)
γ (deg)	93.513(2)	90
V (Å^3)	577.64(14)	2634.37(15)
Z	2	4
D_c (g cm^{-3})	3.975	1.946
μ (Mo$K\alpha$) (mm^{-1})	29.424	1.768
F(000)	612	1592
Reflections collected	2992	4198
Independent reflections	2012 ($R_{int} = 0.0542$)	2315 ($R_{int} = 0.0527$)
Observed reflections [$I > 2\sigma(I)$]	1631	1603
Goodness-of-fit (GOF)	1.089	1.101
R_1/wR_2 [$I > 2\sigma(I)$]	0.0677/0.1662	0.0732/0.1606
R_1/wR_2 (all data)	0.0853/0.1815	0.1170/0.1901

[a] $R_1 = \sum||F_o| - |F_c||/\sum|F_o|$, $wR_2 = \left\{\sum w\left[(F_o)^2 - (F_c)^2\right]^2 \Big/ \sum w\left[(F_o)^2\right]^2\right\}^{1/2}$.

Table 2
Important bond lengths (Å) and angles (deg) for complexes **1** and **2**

Complex **1**			
Pb(1)–O(23)#1	2.382(15)	Pb(1)–O(21)	2.443(16)
Pb(1)–O(12)#2	2.489(18)	Pb(1)–O(13)#3	2.673(16)
Pb(1)–O(23)#4	2.738(15)	Pb(2)–O(13)	2.384(15)
Pb(2)–O(22)	2.417(15)	Pb(2)–O(22)#3	2.516(15)
Pb(2)–O(21)#5	2.721(16)	Pb(2)–N(1)	2.729(18)
Pb(1)–O(2)	2.947(22)	Pb(1)–O(11)#4	3.001(15)
Pb(1)–O(22)	2.937(15)	Pb(2)–O(2)	2.899(21)
Pb(2)–O(11)#4	2.997(16)	Pb(2)–O(12)#4	3.057(19)
Hydrogen bonding			
O(1)···O(1)#6	2.472(40)	O(1w)···O(12)	2.742(30)
O(23)#1–Pb(1)–O(21)	82.0(5)	O(23)#1–Pb(1)–O(12)#2	75.5(6)
O(21)–Pb(1)–O(12)#2	79.2(6)	O(23)#1–Pb(1)–O(13)#3	71.4(5)
O(21)–Pb(1)–O(13)#3	105.6(5)	O(12)#2–Pb(1)–O(13)#3	145.3(5)
O(23)#1–Pb(1)–O(23)#4	81.8(5)	O(21)–Pb(1)–O(23)#4	160.7(5)
O(12)#2–Pb(1)–O(23)#4	86.6(6)	O(13)#3–Pb(1)–O(23)#4	78.9(5)
O(13)–Pb(2)–O(22)	81.6(5)	O(13)–Pb(2)–O(22)#3	77.1(5)
O(22)–Pb(2)–O(22)#3	70.6(6)	O(13)–Pb(2)–O(21)#5	72.1(5)
O(22)–Pb(2)–O(21)#5	144.7(5)	O(22)#3–Pb(2)–O(21)#5	80.7(5)
O(13)–Pb(2)–N(1)	72.0(5)	O(22)–Pb(2)–N(1)	70.5(5)
O(22)#3–Pb(2)–N(1)	132.9(5)	O(21)#5–Pb(2)–N(1)	120.5(5)
Complex **2**			
Ni–O(2)	2.028(6)	Ni–O(2w)	2.030(6)
Ni–O(21)	2.056(6)	Ni–O(11)	2.090(6)
Ni–O(1w)	2.097(6)	Ni–N(1)	2.145(7)
P(1)–O(13)	1.492(7)	P(1)–O(11)	1.501(7)
P(1)–O(12)	1.576(6)	P(2)–O(21)	1.478(7)
P(2)–O(22)	1.480(7)	P(2)–O(23)	1.590(7)
C(4)–O(1)	1.276(10)	C(4)–O(2)	1.300(11)
Hydrogen bonding			
O(1)···N(2)	2.757(11)	O(12)···O(22)#2	2.642(9)
O(23)···O(13)#3	2.582(10)	O(1w)···O(22)#4	2.767(8)
O(2w)···O(1)#5	2.687(9)	O(2w)···O(13)#6	2.649(9)
O(12)–H(12a)···O(22)#2	168.0	O(23)–H(23a)···O(13)#3	157.9
O(1)···H(02c)–N(2)	153.4		
O(2)–Ni–O(2w)	86.7(2)	O(2)–Ni–O(21)	92.9(2)
O(2w)–Ni–O(21)	94.6(2)	O(2)–Ni–O(11)	90.0(2)
O(2w)–Ni–O(11)	95.4(2)	O(21)–Ni–O(11)	169.8(2)
O(2)–Ni–O(1w)	177.0(2)	O(2w)–Ni–O(1w)	90.8(2)
O(21)–Ni–O(1w)	89.0(2)	O(11)–Ni–O(1w)	88.5(2)
O(2)–Ni–N(1)	84.0(3)	O(2w)–Ni–N(1)	170.7(2)
O(21)–Ni–N(1)	87.0(3)	O(11)–Ni–N(1)	83.6(3)
O(1w)–Ni–N(1)	98.4(3)		

Symmetry transformations used to generate equivalent atoms:
For complex **1**: #1, $-x+1$, $-y$, $-z+1$; #2, $x-1$, $y-1$, z; #3, $-x+1$, $-y+1$, $-z+1$; #4, $x-1$, y, z; #5, x, $y+1$, z; #6 $-x$, $-y$, $-z$.
For complex **2**: #1, $-x+1/2$, $-y+5/2$, $-z+1$; #2, x, $1-y$, $-1/2+z$; #3, x, $2-y$, $1/2+z$; #4, $1-x$, $1-y$, $1-z$; #5, $1/2-x$, $-1/2+y$, $1/2-z$; #6, x, $-1+y$, z.

2.899(21)–3.001(15) Å, which are too large to be considered as coordination bonds, however they are necessary to saturate the bond valences of the Pb(II) ion [20]. The carboxylate group of the ligand remains non-coordinated, however, O(2) is 2.947(22) and 2.899(21) Å, respectively, from Pb(1) and Pb(2), these large Pb–O distances are resulted from the repulsion of the lone pair electrons with the electrons of the phosphonate oxygen atoms. Each ligand chelates with a Pb(2) tridentately (N(1), O(22) and O(13)) and it also bridges with five Pb(1) and two other Pb(2) ions (Fig. 1). The phosphonate group containing P(2) is hexadentate, bridging with six lead(II) ions (3 Pb(1) and 3 Pb(2)), all three phosphonate oxygen atoms are bidentate metal linkers. The other phosphonate group bridges with three lead(II) ions. O(13) is a μ^2 metal linker and O(11) remains non-coordinated. Based on the charge balance, each ligand should carry four negative charges. Thus the ligand should be 1H-protonated, O(11) atom with a long P–O distance is protonated (Table 2).

The bridging of the above two types of lead(II) ions by phosphonate groups results in a $\langle 002 \rangle$ double layer

with the non-coordinated carboxylate group as a pendant group (Fig. 2). These double layers are further interlinked via hydrogen bonds between the carboxylate groups from two different layers into a 3D network (Fig. 3). The O(1)···O(1a) (symmetry operator: $-x$, $-y$, $-z$) separation is 2.472(40) Å, indicating that the hydrogen bond formed between two carboxylate groups is very strong.

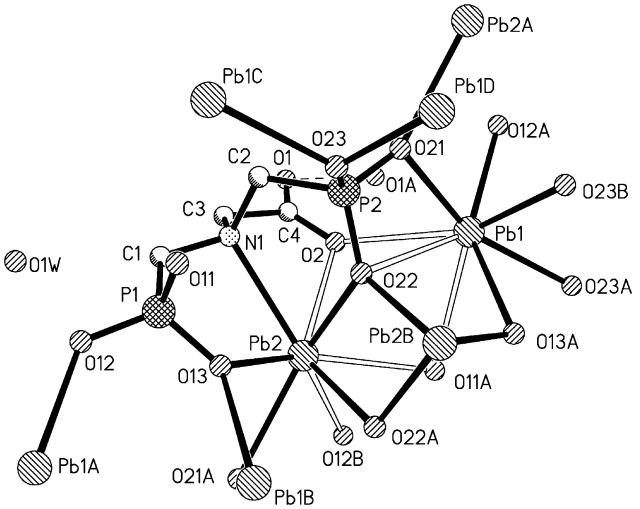

Fig. 1. Asymmetric unit of complex **1**. Hydrogen bonds are represented by dotted lines. Longer Pb–O contacts are drawn as open lines.

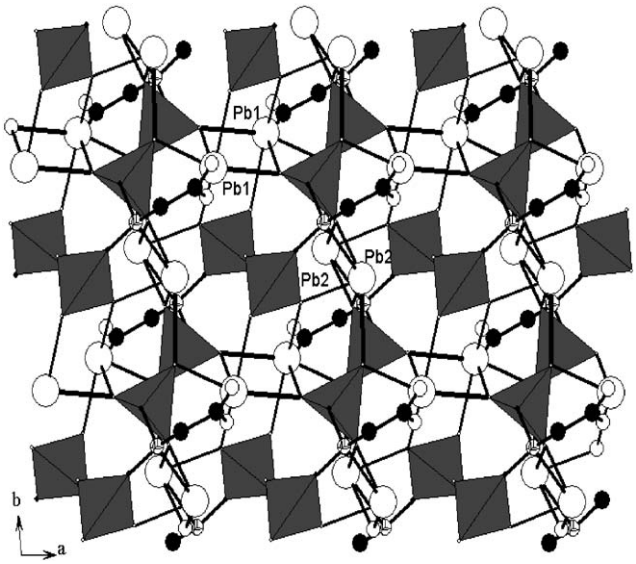

Fig. 2. A $\langle 002 \rangle$ lead(II) carboxylate-phosphonate double layer of complex **1**. C–PO_3 tetrahedra are shaded in dark gray. Pb, N, C and O atoms are represented by open (large), octand, black and open (small) circles, respectively.

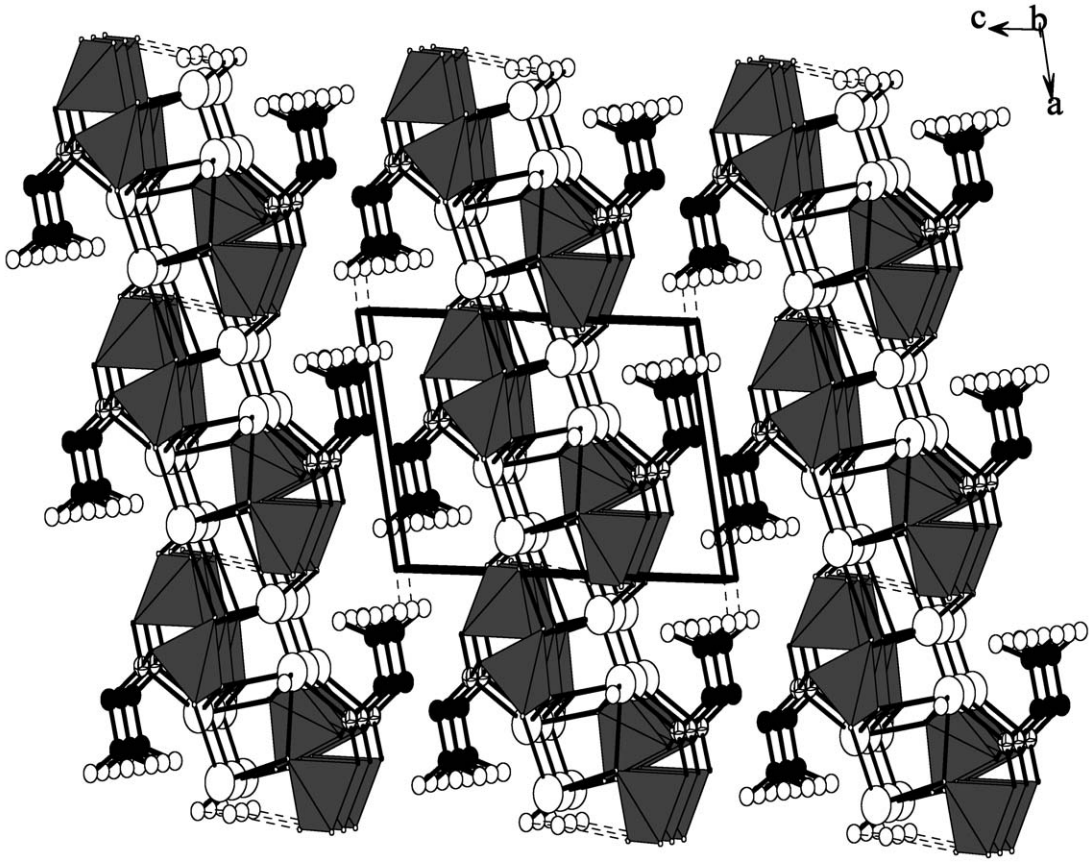

Fig. 3. View of the structure of complex **1** down the *b*-axis. C–PO_3 tetrahedra are shaded in dark gray. Pb, N, C and O atoms are represented by open (large), octand, black and open (small) circles, respectively. Hydrogen bonds are drawn as dotted lines.

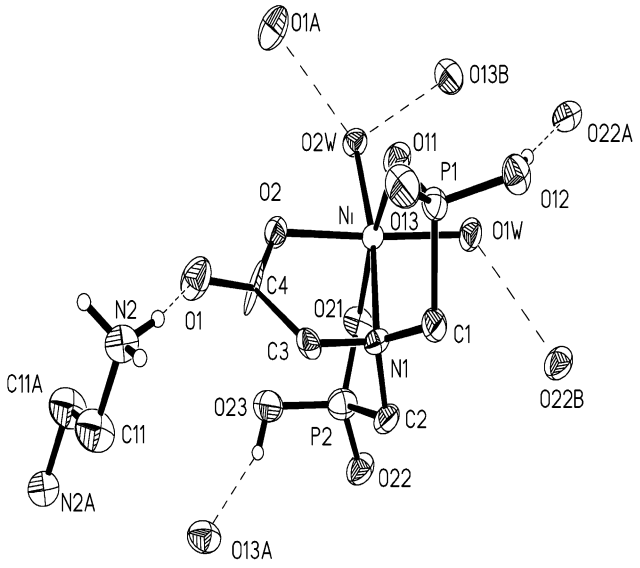

Fig. 4. ORTEP representation of the asymmetry unit of complex **2**. Thermal ellipsoids are drawn at 50% probability. Hydrogen bonds are drawn as dashed lines.

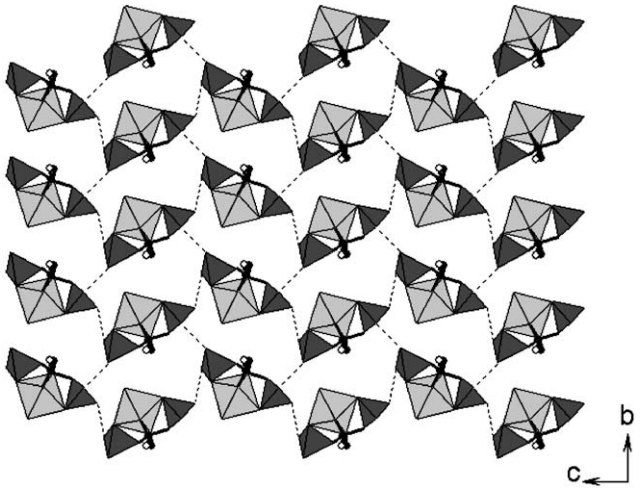

Fig. 5. A 〈800〉 hydrogen bonded 2D layer in complex **2**. The nickel(II) octahedra and C–PO_3 tetrahedra are shaded in dark and light gray, respectively. C and O atoms are represented by black and open circles, respectively. Hydrogen bonds are drawn as dotted lines.

Complex **2** was synthesized by hydrothermal reaction of $NiCl_2 \cdot 6H_2O$, *N*,*N*-bis(phosphonomethyl)aminoacetic acid, 1,2,3-benzenetricarboxylic acid and enthylene diamine at pH = 6. We initially attempted to synthesize mixed-ligand Ni(II) carboxylate-phosphonate, but was unsuccessful. We have been successfully incorporated 1,3,5-benenetricarboxylate in other layered lead(II) diphosphonates, in which the tricarboxylate ligand acts as a pendant group or an intercalated guest molecule between the two layers. The structure of complex **2** features a hydrogen-bonded 2D layer built from molecular units. As shown in Fig. 4, the nickel(II) ion is octahedrally coordinated by two phosphonate oxygen atoms (O(11), O(21), one nitrogen (N(1)) and one carboxylate oxygen (O(2) atom of a tetradentate chelating ligand and two aqua ligands. The Ni–O distances range from 2.028(6) to 2.097(6) Å, and the Ni–N distance is slightly longer than those of Ni–O (2.145(7) Å). These Ni–N and Ni–O distances are comparable to those reported in other nickel(II) phosphonate [19]. Unlike that in complex **1**, the ligand in complex **2** only chelates with a metal ion tetradentately. One carboxylate and four phosphonate oxygen atoms of the ligand remain non-coordinated and are involved in hydrogen bonding. Based on the P–O distances as well as the coordination mode of the ligand, O(12) and O(23) atoms are protonated. Each nickel(II) phosphonate chelating unit is expected to carry a negative charge, thus two such units are needed to balance the two positive charges provided by a 2H-protonated ethylenediamine cation.

The above nickel(II) phosphonate chelating anions are further interconnected into a 〈800〉 2D layer via hydrogen bonds between non-coordinated phosphonate oxygen atoms (Table 2, Fig. 5). A similar hydrogen-bonded 2D layer built from nickel(II) amino-diphosphonate molecular units has been reported previously by our group [18]. The O(12)···O(22) and O(23)···O(13) separations are 2.642(9) and 2.582(10) Å, respectively, and the bond angles for O(12)–H(12a)···O(22) and O(23)–H(23a)···O(13) are 168.0° and 157.9°, respectively (Fig. 4, Table 2). Within the 2D layer, hydrogen bonds are also formed among the aqua ligands and non-coordinated phosphonate oxygen atoms.

It is interesting to note that the protonated ethylenediamine cations are intercalated between a pair of hydrogen-bonded 2D layers, resulting in the formation of a hydrogen-bonded double layer with the 2H-protonated ethylenediamine cations in-between (Fig. 6). Each ethylenediamine cation forms two hydrogen bonds between the amine groups and non-coordinated carboxylate oxygen atoms. The N(2)···O(1) contact is 2.757(11) Å and N(2)–H(02c)···O(1) bond angle is 153.4°. These double layers are held together by weak Van de Waals forces (Fig. 6).

Similar to *N*-(phosphonomethyl)iminodiacetic acid (H_4PMIDA) [10–13], *N*,*N*-bis(phosphonomethyl)aminoacetic acid can adopt a variety of coordination modes and form metal carboxylate-phosphonates with different structural types. So far its Pt(II), Zn(II), Pb(II) and Ni(II) complexes have been isolated, the coordination modes of the ligand are summarized in Scheme 1. The ligand occurs in a zwitterionic form, i.e. one proton on a phosphonate group has been transferred to the amine group [21]. Upon its reaction with Pt(II) ion, it forms a five-membered chelating ring using the nitrogen and the acetate group (Scheme 1a), whereas both phosphonate groups are non-coordinated and the resultant complex is mononuclear [16b]. When Zn(II) ion was used, the metal

phosphonate formed has a 3D network structure, in which the ligand is octadentate and bridges with eight metal ions, and its amine group remains protonated (Scheme 1b) [16a]. In the layered Pb(II) complex, the ligand is decadentate, it chelates with a metal ion tridentately and bridges with seven other metal ions, the carboxylate group remains non-coordinated and one phosphonate group is 1H-protonated (Scheme 1c). The ligand in the mononuclear Ni(II) complex is tetradentately chelating with a metal ion, each of its phosphonate groups is unidentate and 1H-protonated, one of the carboxylate oxygen atoms remains non-coordinated (Scheme 1d). The molecular units of complex **2** are interconnected into a hydrogen bonded 2D layer via hydrogen bonding between non-coordinated phosphonate oxygen atoms.

The XRD powder patterns for complexes **1** and **2** were collected on a Philips X'Pert-MPD diffractometer using graphite-monochromated Cu$K\alpha$ radiation in the angular range $2\theta = 5-70°$. Their powder patterns match with the ones calculated from their single crystal structure data, thus both compounds exist as a single phase.

IR spectra for complexes **1** and **2** were recorded in the region from 4000 to 400 cm^{-1} and can be used to study in detail the hydration water and the P–O–H groups. The broad band at 3438 and 3257 cm^{-1} for complex **1** can be assigned to the O–H stretching vibrations, such band appearing at 3184 cm^{-1} for complex **2** is more intense. The peak at 1651 cm^{-1} for complex **1** may be due to an overtone or combination band of the CPO_3 stretching vibrations [17c]. The sharp band at 1627 cm^{-1} for complex **2** is due to the bending H–O–H vibration of the hydration water. The two bands at 2734 and 2305 cm^{-1} for complex **2** are probably due to υ(P–OH) and 2δ(P–O–H), respectively, are characteristic of hydrogen phosphonate groups [17c], however, they are too weak to be observed for complex **1**.

The TGA curve of complex **1** shows two major weight losses (Fig. 7). The first step is the release of one lattice water molecule that started at 72°C, the second step, the pyrolysis of the organic ligand, was complete at about 780°C. The final products are $Pb_2P_2O_7$. The total weight loss of 13.0% is in good agreement with the calculated value (14.9%). After that there is a slight weight gain (<2.0%) starting from 800°C, indicating that some of the lead(II) ions have been oxidized. There are two main steps of weight losses for complex **2**. The first step started from 155°C and completed at 450°C, which involves in the release of four aqua ligands, one ethylenediamine molecule and two water molecules

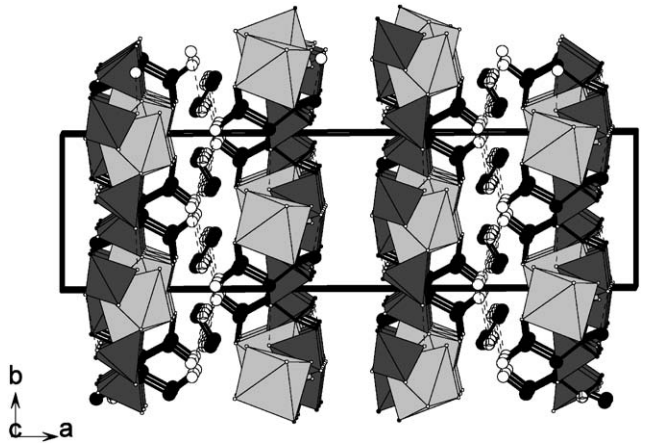

Fig. 6. View of the structure of complex **2** down the *c*-axis. The nickel(II) octahedra and C–PO_3 tetrahedra are shaded in dark and light gray, respectively. N, C and O atoms are represented by octand, black and open circles, respectively. Hydrogen bonds are drawn as dotted lines.

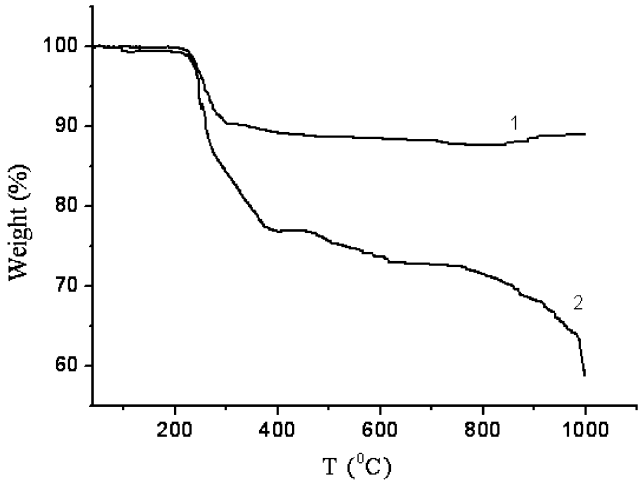

Fig. 7. TGA curves for the Pb(II) (1) and Ni(II) (2) complexes.

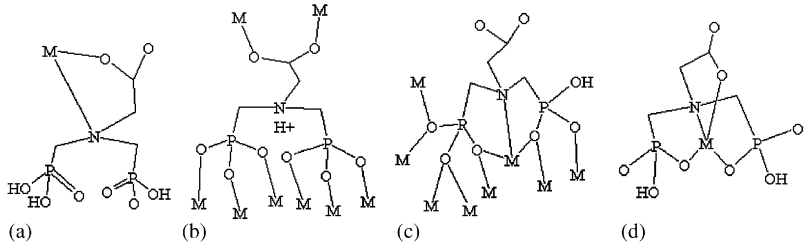

Scheme 1. Coordination modes of the carboxylate-phosphonate ligand in its Pt(II) (a), Zn(II) (b), Pb(II) (c), and Ni(II) (d) complexes.

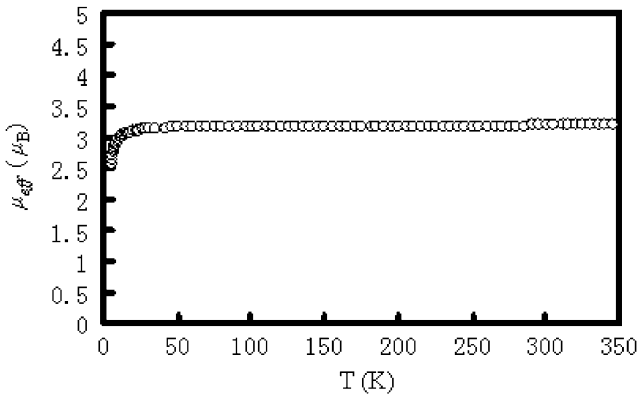

Fig. 8. Plot of the effective magnetic moment (μ_{eff}) versus T for complex **2**.

formed by the condensation of hydrogen phosphonate groups. The observed weight loss of 23.2% is in good agreement with the calculated one (21.8%). The second step corresponds to the decomposition of the phosphonate ligand, which started from 450°C and continued up to 1000°C. The final product is $Ni(PO_3)_2$, a metal metaphosphate. The total weight loss of 40.7% is a bit less than the calculated value (43.8%), which means that the decomposition process is not complete at 1000°C as also evidenced by the slope of the TGA curve.

The results of the magnetic susceptibility measurements for the Ni(II) complex at $1T$, $3T$ and $5T$ are identical and those of $5T$ are shown in Fig. 8. At room temperature the measured μ_{eff} of 3.2 μ_B corresponds to a nickel(II) ion ($S = 1$, $g \approx 2.26$). At 5 K, the μ_{eff} value decreases to 2.56 μ_B. The measured Curie constant and the θ value are 1.292 emu K/mol and –4.4 K, respectively. Thus there is weak antiferromagetic interaction between Ni(II) ions from neighboring chelating units. The shortest Ni···Ni separation is 6.971(1) Å.

5. Conclusions

Hydrothermal reactions of *N*,*N*-bis(phosphonomethyl)aminoacetic acid ($HO_2CCH_2N(CH_2PO_3H_2)_2$) with metal(II) salts afforded two new metal carboxylate-phosphonates, namely, $Pb_2[O_2CCH_2N(CH_2PO_3)(CH_2PO_3H)]\cdot H_2O$ **1** and $\{NH_3CH_2CH_2NH_3\}\{Ni[O_2CCH_2N(CH_2PO_3H)_2][H_2O]_2\}$ **2**. The structure of complex **1** features a $\langle 002 \rangle$ lead(II) carboxylate-phosphonate double layer with the non-coordinated carboxylate groups as the pedant groups. The double layers are further interlinked via hydrogen bonds between the carboxylate groups to form a 3D network. The structure of complex **2** contains a $\langle 800 \rangle$ hydrogen-bonded 2D layer built from $\{Ni[O_2CCH_2N(CH_2PO_3H)_2][H_2O]_2\}^-$ anions that are interlinked by hydrogen bonds between non-coordinated phosphonate oxygen atoms, with the 2H-protonated ethylenediamine cations being intercalated between two layers, forming hydrogen bonds with the non-coordinated carboxylate oxygen atoms.

Acknowledgments

This work was supported by the Innovative Project and the Introduction of Overseas Elitists Program by Chinese Academy of Sciences, and the Scientific Research Foundation for the Returned Overseas Chinese Scholars, State Education Ministry. We thank Ms. Eva Brücher for the magnetic measurements.

References

[1] (a) E.W. Stein Sr., A. Clearfield, M.A. Subramanian, Solid State Ionics 83 (1996) 113;
(b) G. Alberti, U. Costantino, in: J.M. Lehn (Ed.), Comprehensive Supramolecular Chemistry, Pergamon-Elsevier Science Ltd., London, 1996, p. 1;
(c) A. Clearfield, Curr. Opin. Solid State Mater. Sci. 1 (1996) 268;
(d) A. Clearfield, Metal phosphonate chemistry, in: K.D. Karlin (Ed.), Progress in Inorganic Chemistry, Vol. 47, Wiley, New York, 1998, pp. 371–510 (and references herein).
[2] M.E. Thompson, Chem. Mater. 6 (1994) 1168.
[3] G. Alberti, U. Costantino, in: J.M. Lehn (Ed.), Comprehensive Supramolecular Chemistry, Pergamon-Elsevier Science Ltd., London, 1996, p. 151.
[4] (a) A.K. Cheetham, G. Ferey, T. Loiseau, Angew. Chem. Int. Ed. 38 (1999) 3268;
(b) J. Zhu, X. Bu, P. Feng, G.D. Stucky, J. Am. Chem. Soc. 122 (2000) 11563.
[5] (a) B. Zhang, A. Clearfield, J. Am. Chem. Soc. 119 (1997) 2751;
(b) A. Clearfield, C.V.K. Sharma, B. Zhang, Chem. Mater. 13 (2001) 3099;
(c) J.-G. Mao, Z. Wang, A. Clearfield, Inorg. Chem. 41 (2002) 3713.
[6] H.L. Ngo, W. Lin, J. Am. Chem. Soc. 124 (2002) 14298.
[7] (a) F. Fredoueil, M. Evain, D. Massiot, M. Bujoli-Doeuff, P. Janvier, A. Clearfield, B. Bujoli, J. Chem. Soc. Dalton Trans. (2002) 1508;
(b) P. Rabu, P. Janvier, B. Bujoli, J. Mater. Chem. 9 (1999) 1323;
(c) S. Drumel, P. Janiver, P. Barboux, M. Bujoli-Doeuff, B. Bujoli, Inorg. Chem. 34 (1995) 148.
[8] (a) N. Stock, S.A. Frey, G.D. Stucky, A.K. Cheetham, J. Chem. Soc. Dalton Trans. (2000) 4292;
(b) S. Ayyappan, G.D. de Delgado, A.K. Cheetham, A.K., G. Ferey, C.N.R. Rao, J. Chem. Soc. Dalton Trans. (1999) 2905;
(c) A. Distler, S.C. Sevov, Chem. Commun. (1998) 959.
[9] R. Vivani, U. Costantino, M. Nocchetti, J. Mater. Chem. 12 (2002) 3254.
[10] (a) B. Zhang, D.M. Poojary, A. Clearfield, G.-Z. Peng, Chem. Mater. 8 (1996) 1333;
(b) D.M. Poojary, A. Clearfield, J. Organomet. Chem. 512 (1996) 237;
(c) D.M. Poojary, B. Zhang, A. Clearfield, Angew. Chem. Int. Ed. 33 (1994) 2324.
[11] B. Zhang, D.M. Poojary, A. Clearfield, Inorg. Chem. 37 (1998) 249.
[12] (a) J.-G. Mao, A. Clearfield, Inorg. Chem. 41 (2002) 2319;
(b) J.-G. Mao, Z. Wang, A. Clearfield, Inorg. Chem. 41 (2002) 6106.

[13] S.O.H. Gutschke, D.J. Price, A.K. Powell, P.T. Wood, Angew. Chem. Int. Ed. 38 (1999) 1088.
[14] (a) J.-G. Mao, C. Lei, Y.-Q. Sun, H.-Y. Zeng, A. Clearfield, Inorg. Chem. 42 (2003) 6157;
(b) D.S. Sagatys, C. Dahlgren, G. Smith, R.C. Bott, J.M. White, J. Chem. Soc. Dalton Trans. (2000) 3404;
(c) E. Galdecka, Z. Galdecki, P. Gawryszewska, J. Legendziewicz, New J. Chem. 24 (2000) 387.
[15] (a) A. Turner, P.A. Jaffrès, E.J. MacLean, D. Villemin, V. McKee, G.B. Hix, Dalton Trans. (2003) 1314;
(b) N. Stock, Solid State Sci. 4 (2002) 1089.
[16] (a) J.-G. Mao, Z. Wang, A. Clearfield, New J. Chem. 26 (2002) 1010;
(b) M. Galanski, B.K. Keppler, B. Nuber, Angew. Chem. Int. Ed. 34 (1995) 1103.
[17] (a) A. Cabeza, M.A.G. Aranda, M. Martinez-Lara, S. Bruque, J. Sanz, Acta Crystallogr. B 52 (1996) 982;
(b) D.M. Poojary, B.L. Zhang, A. Cabeza, M.A.G. Aranda, S. Bruque, A. Clearfield, J. Mater. Chem. 6 (1996) 639;
(c) A. Cabeza, M.A.G. Aranda, S. Bruque, J. Mater. Chem. 9 (1999) 571;
(d) B. Adair, S. Natarajan, A.K. Cheetham, J. Mater. Chem. 8 (1998) 1477;
(e) N. Stock, G.D. Stucky, A.K. Cheetham, Chem. Commun. (2000) 2277.
[18] G.M. Sheldrick, SHELXTL, Crystallographic Software Package, Version 5.1, Bruker-AXS, Madison, WI, 1998.
[19] J.-G. Mao, Z. Wang, A. Clearfield, J. Chem. Soc. Dalton Trans. (2002) 4541.
[20] M.R.St.J. Foreman, T. Gelbrich, M.B. Hursthouse, M.J. Plater, Inorg. Chem. Commun. 3 (2000) 234.
[21] L.M. Shkol'nikova, A.A. Masyuk, F.F. Khizbullin, B.P. Strunin, S.S. Sotman, B.V. Zhadanov, M.V. Rudomino, N.M. Dyatlova, Zh. Struct. Khim. 31 (1990) 81.